

Statistics of Semiflexible Polymer Chains and the Generalized Borel Transform

Marcelo Marucho and Gustavo A. Carri^{yz}

*The Maurice Morton Institute of Polymer Science,
The University of Akron, Akron, OH 44325-3909, USA.*

Abstract

In this paper, we present a new approach to the discrete version of the Wormlike Chain Model (WCM) of semiflexible polymers. Our solution to the model is based on a new computational technique called the Generalized Borel Transform (GBT) which we use to study the statistical mechanics of semiflexible polymer chains. Specifically, we evaluate the characteristic function of the model approximately. Afterward, we compute the polymer propagator of the model using the GBT and find an expression valid for polymers with any number of segments and values of the semiflexibility parameter. This expression captures the limits of flexible and infinitely stiff polymers exactly. In between, a smooth and approximate crossover behavior is predicted. Another property of our propagator is that it fulfills the condition of finite extensibility of the polymer chain. We have also calculated the single chain structure factor. This property is a decreasing function of the wave vector, k ; until a plateau is reached. Our computations clearly show that the structure factor decreases faster with increasing wave vector when the semiflexibility parameter is increased. Furthermore, when the wave vector is large enough, there is a regime where the structure factor follows an approximate power law of the form $k^{-\alpha}$ even for short polymer chains. α is equal to two for flexible polymers and to one for rigid chains. We also compare our results to the predictions of other models.

^y To whom any correspondence should be addressed
Electronic address: marucho@polymer.uakron.edu

^zElectronic address: carri@polymer.uakron.edu

I. INTRODUCTION

In recent years, experimental studies of biological macromolecules have motivated intense research in the field of statistical mechanics of single semiflexible polymer chains. Indeed, studies like force-elongation measurements of different biological (DNA, titin, tenascin) and synthetic (polyethylene glycol, polyvinyl alcohol) polymers using Atomic Force Microscopes, Optical Tweezers and other recently developed tools are abundant[1]. The measured force-elongation curve is generally fitted to the prediction of the Wormlike Chain Model (WCM) of semiflexible chains[2], originally proposed by Kratky and Porod[3]. From this fit, parameters like the persistence length of the biopolymer are extracted. Another kind of experiments has targeted the mechanical properties of eukaryotic cells[4]. These properties are determined by an assembly of protein fibers called the cytoskeleton. This three dimensional assembly is made of the cytoskeletal polymers (microtubules, actin filaments, etc.). All these polymers are semiflexible polymers at the relevant length scales (a few microns at most). Thus, the predictions of the WCM are very relevant for the understanding of the physical behavior of cytoskeletal polymers.

The WCM was originally proposed by Kratky and Porod in 1949[3] and reformulated using field theoretic methods by Saito *et al.*[5] in 1967. In this model, the polymer chain displays resistance to bending deformations. This resistance is modeled using a free energy that penalizes bending the polymer backbone. The free energy depends on parameters (elastic constants) that are a consequence of many short-range monomer-monomer interactions. Explicitly, the free energy is

$$-\frac{\kappa}{2} \int_0^L ds \frac{d^2 \mathbf{R}(s)}{ds^2} \cdot \frac{d^2 \mathbf{R}(s)}{ds^2}; \quad (1)$$

where $\mathbf{R}(s)$ is the vectorial field that represents the polymer chain, s is the arc of length parameter, L is the contour length of the polymer and κ is the bending modulus. In addition, the local inextensibility constraint $|\frac{d\mathbf{R}(s)}{ds}| = 1$ must be satisfied. As a consequence of the bending rigidity, a wormlike chain is characterized by a persistence length (proportional to the bending modulus) such that, if the length scale is shorter than the persistence length, then the chain behaves like a rod while, if the length scale is larger than the persistence length, then the chain is governed by the configurational entropy that favors the random-

walk conformations.

The local inextensibility constraint has not allowed researchers to find an exact solution to the WCM. Indeed, the constraint $\int d\mathbf{R}(\mathbf{s}) = d\mathbf{s}j = 1$ is written using a Dirac delta distribution in infinite dimensions. Depending on how the constraint is written, $\int d\mathbf{R}(\mathbf{s}) = d\mathbf{s}j = 1$ or $(d\mathbf{R}(\mathbf{s}) = d\mathbf{s})^2 = 1$, we get an Edwards Hamiltonian that is non-analytic or non-linear, respectively. Consequently, there is no exact solution of this model at present. However, a few properties like the first few moments of the distribution of the end-to-end distance[5, 6] are known exactly.

The aforementioned complexity of the WCM has motivated many approximate treatments of semiflexible polymers. For example, Fixman and Kovac[7] developed a modified Gaussian model for stiff polymer chains under an external field (external force). In this approach, they computed an approximate distribution for the bond vectors from which they were able to compute the partition function and average end-to-end vector. An alternative approach was proposed by Harris and Hearst[8] who developed a distribution for the continuous model from which they were able to compute the two-point correlation function and, consequently, the mean-square end-to-end distance and radius of gyration. Another statistical property of interest has been the distribution function of the end-to-end distance or its Fourier transform. Many approximations for this function have been proposed. For example, different expansions of the distribution in inverse powers of the number of segments have been developed[9, 10]. Similarly, perturbations with respect to the rodlike limit have been derived[11]. Other approaches to the distribution function of the end-to-end distance of semiflexible polymers have led to modified Gaussian functions[12, 13]. Finally, many approximations have been proposed for the structure factor[14, 15].

As stated in the previous paragraph, most of the approximate treatments of the distribution function of the end-to-end distance have been perturbative in nature. Indeed, these approximations were perturbation expansions with respect to the flexible or rigid chain limits. A different approach to semiflexible polymers was taken by Kholodenko[16, 17, 18]. In this model, the Euclidean version of the Dirac propagator is used to predict the conformational properties of semiflexible polymers. In particular, the single chain structure factor has been used to describe experimental data quantitatively[19]. Recently, Winkler has proposed another treatment of semiflexible polymers[20]. In this work, an approximate expression for

the distribution function valid for any value of the stiffness of the polymer backbone was developed using the Maximum Entropy Principle.

Motivated by the experimental studies done on semiflexible polymers and our incomplete understanding of the properties of the WCM, we have developed a new approach that captures many physical properties of the model, like the limits of flexible and rigid polymers, exactly and provides approximate crossover behaviors for all the distribution functions. To accomplish this goal, we have employed a computational technique called the Generalized Borel Transform (GBT) which was taken from Quantum Mechanics and Quantum Field Theories[21, 22, 23]. This method computes Mellin/Laplace transforms exactly. We provide a brief summary of this technique in Appendix A.

This paper is organized as follows. In section II, we evaluate the characteristic function of the WCM approximately such that some physical constraints are satisfied exactly. Furthermore, we evaluate the distribution function (polymer propagator) using the GBT and compute the single chain structure factor. In Section III we discuss the results of our calculations which are valid for any value of the semiflexibility of the polymer. Section IV contains the conclusions of our work and some speculations about applications to polymer physics of possible extensions of the GBT. The details of the mathematical calculations are presented in the appendices.

II. THEORY

A. The Model and Evaluation of the Characteristic Function

Consider a polymer chain modeled as a sequence of n bond vectors $(\mathbf{R}_1; \mathbf{R}_2; \dots; \mathbf{R}_n)$ connected in a sequential manner. In addition, let us assume that the length of each bond vector is 1 (=Kuhn length) and that pairs of consecutive bond vectors try to be parallel to each other. This preferential orientation is modeled with a Boltzmann weight given by the following expression [7, 13, 14, 24]

$$\exp \left[-\frac{1}{2} \sum_{i=1}^{n-1} (\mathbf{R}_{i+1} - \mathbf{R}_i)^2 \right] \quad (2)$$

where β is the strength of the interaction in units of thermal energy ($\beta = k_B T$). Inserting Eq. (2) into the expression for the propagator of the Random Flight Model[25], we obtain the following expression for the polymer propagator of semiflexible chains

$$P(\mathbf{R}; n; \beta) = \int d\mathbf{R}_k g^{(n)}(\mathbf{R}_j) \exp\left(-\beta \sum_{j=1}^n \mathbf{R}_j \cdot \mathbf{R}_{j+1}\right) \quad (3)$$

where \mathbf{R} is the end-to-end vector and \mathbf{R}_j is given by the formula

$$\mathbf{R}_j = \frac{(\mathbf{R} \cdot \mathbf{j})}{4l^2} \quad (4)$$

The propagator, Eq. (3), is not normalized.

We proceed to express the delta function using its Fourier representation[26] then, Eq. (3) becomes

$$P(\mathbf{R}; n; \beta) = \int \frac{d^3k \exp(-i\mathbf{R} \cdot \mathbf{k})}{(2\pi)^3 (4l^2)^n} \int d\mathbf{R}_k g^{(n)}(\mathbf{R}_j) \exp\left(-\beta \sum_{j=1}^n \mathbf{R}_j \cdot \mathbf{k} + \sum_{i=1}^{n-1} \mathbf{R}_{i+1} \cdot \mathbf{k}\right) \quad (5)$$

which can be used to define the characteristic function, $K(\mathbf{k}; n; l)$, as follows

$$P(\mathbf{R}; n; \beta) = \int \frac{d^3k}{(2\pi)^3} \exp(-i\mathbf{R} \cdot \mathbf{k}) K(\mathbf{k}; n; l) \quad (6)$$

The mathematical expression of the characteristic function is

$$K(\mathbf{k}; n; l) = \frac{1}{(4l^2)^n} \int d\mathbf{R}_k g^{(n)}(\mathbf{R}_j) \exp\left(-\beta \sum_{j=1}^n \mathbf{R}_j \cdot \mathbf{k} + \sum_{i=1}^{n-1} \mathbf{R}_{i+1} \cdot \mathbf{k}\right) \quad (7)$$

Note that since the polymer propagator, Eq. (3), is not normalized then the characteristic function, Eq. (7), does not approach one when the wave vector goes to zero. Instead, it approaches the canonical partition function of the model. Furthermore, note that the characteristic function is a Fourier Transform in a $3n$ -dimensional space.

As stated before by Yamakawa[6], the exact evaluation of the characteristic function (or the polymer propagator) for semiflexible chains is not possible at present. Therefore, we have developed a new approximation to evaluate this function. This new mathematical approach

was developed in such a way that the most relevant physics of the problem is not altered by the approximation. Specifically, the proposed approach keeps the thermodynamics (partition function) of the model exact. Moreover, all the properties of fully flexible chains ($\beta \rightarrow 0$) and infinitely stiff chains ($\beta \rightarrow \infty$) are preserved exactly. Consequently, this approach captures both asymptotic limits exactly and provides an approximate description of the crossover behavior. In addition, our treatment of the problem uses the exact expression of the mean-square end-to-end distance. Consequently, this quantity and the mean-square radius of gyration are exact. Another important property of our approach is that it keeps the local inextensibility constraint intact. Therefore, our chains have finite extensibility and this model can be used to compute the force-elongation relationship of semiflexible polymers. We describe our approximation hereafter.

Let us start by computing the following class of integrals

$$G_j = \int_0^Z dR_j (\mathcal{R}_j - 1) \exp(i\mathbf{R}_j \cdot \mathbf{k} + \mathbf{R}_{j+1} \cdot \mathbf{R}_j); \quad (8)$$

which are present in the characteristic function. The wave vector \mathbf{k} is constant and can be chosen in the direction of the versor $\hat{\mathbf{z}}$. Writing all the vectors in spherical coordinates we can express G_j as follows

$$G_j = \int_0^Z d(\mathcal{R}_j) \mathcal{R}_j^2 (\mathcal{R}_j - 1) \int_0^Z d\mathcal{R}_{j+1} \sin(\theta_j) \exp(i\mathcal{R}_j \cos(\theta_j) + \mathcal{R}_{j+1} \cos(\theta_{j+1}) \cos(\theta_j)) \int_0^\pi d'\mathcal{R}_j \exp(-\cos(\theta'_j) + \sin(\theta'_j)); \quad (9)$$

where θ_j and θ_{j+1} are defined as follows

$$\begin{aligned} \mathcal{R}_j \mathcal{R}_{j+1} \sin(\theta_j) \cos(\theta'_{j+1}) \sin(\theta_{j+1}); \\ \mathcal{R}_j \mathcal{R}_{j+1} \sin(\theta_j) \sin(\theta'_{j+1}) \sin(\theta_{j+1}); \end{aligned} \quad (10)$$

The θ'_j -integrals can be done exactly. The result is

$$F_j(\theta_j; \theta_{j+1}) = \int_0^Z d\mathcal{R}_j \exp(-\cos(\theta'_j) + \sin(\theta'_j)) = 2 I_0(\mathcal{R}_j \mathcal{R}_{j+1} \sin(\theta_j) \sin(\theta_{j+1})); \quad (11)$$

where $I_0(x)$ is the Bessel function of second class[27]. After we integrate the delta function, the function G_j becomes

$$G_j = 2^{-1} \int_0^Z d_j \sin(\theta_j) \exp \left[i \left(\sum_{k=1}^{j-1} k \cos(\theta_{k+1}) \cos(\theta_j) \right) \right] I_0 \left(\sum_{k=1}^{j-1} k \sin(\theta_j) \sin(\theta_{k+1}) \right) : \quad (12)$$

We now replace this expression into Eq. (7) and obtain the characteristic function

$$K(k; n; l) = 2^{-n} \int_0^Z d_n \sin(\theta_n) \exp \left[i \left(\sum_{k=1}^{n-1} k \cos(\theta_{k+1}) \cos(\theta_n) \right) \right] I_0 \left(\sum_{k=1}^{n-1} k \sin(\theta_n) \sin(\theta_{k+1}) \right) : \quad (13)$$

The evaluation of $K(k; n; l)$ is done by iterations. First, we take the term $j = 1$, redefine $j! = k=1$ and $l = l^2$, and remove the factor 2^{-1} from the definition of $G_j(\cdot)$ in Eq. (12); then, we can write

$$G_1(\theta_2) = \int_0^Z d_1 \sin(\theta_1) \exp \left[i \left(\sum_{k=1}^0 k \cos(\theta_{k+1}) \cos(\theta_2) \right) \right] I_0 \left(\sum_{k=1}^0 k \sin(\theta_2) \sin(\theta_{k+1}) \right) : \quad (14)$$

which is exactly doable[28]. The result is

$$G_1(\theta_2) = 2^{-1} \frac{\sinh^2 \left(\frac{k^2 + 2ik \cos(\theta_2)}{2} \right)}{k^2 + 2ik \cos(\theta_2)} : \quad (15)$$

The next step in the iterative process is the evaluation of $G_2(\theta_3)$ given by

$$G_2(\theta_3) = \int_0^Z d_2 \sin(\theta_2) \exp \left[i \left(\sum_{k=1}^1 k \cos(\theta_{k+1}) \cos(\theta_3) \right) \right] I_0 \left(\sum_{k=1}^1 k \sin(\theta_3) \sin(\theta_{k+1}) \right) G_1(\theta_2) : \quad (16)$$

This integral is not exactly doable. Consequently, we proceed to approximate it such that the asymptotic limits of flexible and stiff polymers are captured exactly. Thus, the expression that we obtain will give an approximate crossover behavior between the aforementioned limiting regimes. Note that in the limit of very stiff chains, $l \rightarrow 1$, all the segments will be parallel to each other. In other words, when $l \rightarrow 1$, $\theta_2 \rightarrow \theta_3$. Then, in this limit we can say that

$$G_2(\theta_3) \approx [G_1(\theta_3)]^2 : \quad (17)$$

In the other limit, $l \rightarrow 0$, $G_1(\theta_2)$ is independent of θ_2 . Therefore, Eq. (17) is also valid in the limit of flexible chains. Thus, we conclude that Eq. (17) is a good approximation for

$G_2(\beta)$ since it captures the asymptotic limits exactly and provides an approximate crossover behavior for $G_2(\beta)$.

The iteration of the aforementioned approximation $n - 1$ times leads to the following expression for the characteristic function

$$K(k; \beta; n) = \frac{1}{2^n} \int_0^{2\pi} d\theta \sin(\theta) \exp[ik \cos(\theta)] [G_1(\theta)]^{n-1} : \quad (18)$$

Note that this expression gives the exact canonical partition function of the model

$$Z_n(\beta) = K(0; \beta; n) = \frac{\sinh(\beta)}{\beta} : \quad (19)$$

Thus, this first part of the approximation preserves both asymptotic behaviors and the thermodynamics of the problem intact.

Let us now proceed to evaluate the approximate expression of the characteristic function, $K(k; \beta; n)$. The integral in Eq. (18) is not exactly doable thus, we evaluate it using a variational procedure. Let us introduce the following ansatz

$$\exp\left[-\frac{k^2}{2} + 2ik \cos(\theta)\right] = \exp\left[-\frac{k^2}{2} + \frac{2ikg_m \cos(\theta)}{1 + g_m^2 \cos^2(\theta)}\right]; \quad (20)$$

where the parameters g_m and β_m are determined from the constraints imposed by the physics of the problem as described below. One of the requirements is that the flexible and rigid limits are captured exactly by the model. This requires that the parameters must behave in the following way

$$\begin{aligned} g_m &\rightarrow 0 & \beta_m &\rightarrow 0; & g_m &\rightarrow 1 & \beta_m &\rightarrow 1 : \\ \beta_m &\rightarrow 1 & g_m &\rightarrow 0 & \beta_m &\rightarrow 0 & g_m &\rightarrow 1 : \end{aligned} \quad (21)$$

Using Eq. (20), we can approximate the characteristic function as follows

$$\begin{aligned} K(k; \beta; n) &= \frac{1}{2^n} \int_0^{2\pi} d\theta \sin(\theta) \exp[ik \cos(\theta)] [1 + (n-1)g_m] g_m \\ &\approx \frac{1}{2^n} \int_0^{2\pi} d\theta \sin(\theta) \exp\left[-\frac{k^2}{2} + \frac{2ikg_m \cos(\theta)}{1 + g_m^2 \cos^2(\theta)}\right] [1 + (n-1)g_m] g_m \\ &= \frac{1}{2^n} \int_0^{2\pi} d\theta \sin(\theta) \exp\left[-\frac{k^2}{2} + \frac{2ikg_m \cos(\theta)}{1 + g_m^2 \cos^2(\theta)}\right] [1 + (n-1)g_m] g_m \\ &= \frac{1}{2^n} \int_0^{2\pi} d\theta \sin(\theta) \exp\left[-\frac{k^2}{2} + \frac{2ikg_m \cos(\theta)}{1 + g_m^2 \cos^2(\theta)}\right] [1 + (n-1)g_m] g_m \end{aligned} \quad (22)$$

Note that the term

$$ikg_m \cos(\theta_n) = \frac{q}{2} \frac{1}{k^2 - k_m^2}; \quad (23)$$

goes to zero as $k \rightarrow 1$ in the limit of $k \rightarrow 1$ and, when $k \rightarrow 0$, it also approaches zero because $g_m \rightarrow 0$. Thus, neglecting this term does not alter the predictions of the model for the flexible and stiff limits. Consequently, we approximate Eq. (22) as follows

$$K(k; n) = \frac{\int_0^h \frac{\sinh \frac{nq}{2} \frac{1}{k^2 - k_m^2} \cos \theta_{n-1}}{2 \frac{1}{k^2 - k_m^2} \frac{1}{k^2 - k_m^2} \cos \theta_{n-1}} d\theta_n \sin(\theta_n) \exp[ik \cos(\theta_n) [1 + (n-1)g_m]g]; \quad (24)$$

which is exactly doable. The final expression for the characteristic function is

$$K(k; n) = \frac{\int_0^h \frac{\sinh \frac{nq}{2} \frac{1}{k^2 - k_m^2} \cos \theta_{n-1}}{\frac{1}{k^2 - k_m^2} \frac{1}{k^2 - k_m^2} \cos \theta_{n-1}} \sin \theta_n [1 + (n-1)g_m]g; \quad (25)$$

We note that the expression of the characteristic function given by Eq. (25) recovers the exact expression of the canonical partition function of the model, Eq. (19), in the limit of $k \rightarrow 0$.

Let us now proceed to determine the values of the parameters k_m and g_m from the physics of the problem. We first look at the force-elongation behavior predicted by this model. This curve is given by the following mathematical expression

$$L = \frac{\partial \ln K(iF; n)}{\partial F} = \frac{1}{K(iF; n)} \frac{\partial K(iF; n)}{\partial F}; \quad (26)$$

where F is the applied force and L is the average end-to-end distance of the polymer chain in the direction of the force. The physics of the problem imposes the following constraint

$$\lim_{F \rightarrow 1} \frac{1}{K(iF; n)} \frac{\partial K(iF; n)}{\partial F} = n; \quad (27)$$

which represents the finite extensibility of the polymer chain. In other words, the polymer chain cannot be stretched more than its total contour length. This constraint, as expressed by Eq. (27), results in the following relationship between the parameters k_m and g_m

$$g_{jn} = 1 - \frac{1}{n}; \quad (28)$$

which is in perfect agreement with the required asymptotic behaviors given by Eq. (21).

Equation (28) gives one of the two equations required to determine the parameters χ_{jn} and g_{jn} completely. The second equation is obtained from the mean-square end-to-end distance, $\langle R^2 \rangle_{jn}$. We require that our approximation reproduce this statistical quantity exactly. The exact mathematical expression of this average is [13, 29],

$$\langle R^2 \rangle_{jn}^D = \frac{1}{n} \frac{1 + L(\chi_{jn})}{L(\chi_{jn})} - 2L(\chi_{jn}) \frac{1 - L(\chi_{jn})^n}{(1 - L(\chi_{jn}))^2}; \quad (29)$$

where $L(\chi)$ is the Langevin function [28].

In order to derive the second relationship between χ_{jn} and g_{jn} , we divide the characteristic function, Eq. (25), by the canonical partition function and expand this ratio in powers of the wave vector k to second order. The result is the following

$$\langle R^2 \rangle_{jn}^D = \frac{1}{Z_n(\chi)} \sum_{k=0}^{\infty} \frac{K(k; \chi; n)}{k^2} = [1 + (n-1)g_{jn}]^2 + \frac{3(n-1)^2}{n} L(\chi); \quad (30)$$

which completes our approximation. Equations (28), (29) and (30) determine χ_{jn} and g_{jn} completely. Furthermore, the use of the exact expression for $\langle R^2 \rangle_{jn}$ assures that our approximation predicts not only $\langle R^2 \rangle_{jn}$ exactly, but also $\langle R_g^2 \rangle_{jn}^D$ since they are related by the equation[29]

$$\langle R_g^2 \rangle_{jn} = \frac{1}{(n+1)^2} \sum_{i=1}^n (n-i+1) \langle R^2 \rangle_{j,ni}^D; \quad (31)$$

The final expression for χ_{jn} is

$$\chi_{jn} = \frac{2n(n-1) \frac{1}{4n^2(n-1)^2} + \frac{1}{4(n-1)^2 + \frac{3(n-1)}{n} L(\chi)} - \frac{1}{n^2} \langle R^2 \rangle_{jn}}{2(n-1)^2 + \frac{3(n-1)}{n} L(\chi)}; \quad (32)$$

and our approximation is complete.

B. Evaluation of the Polymer Propagator using the GBT

Replacing the expression given by Eq. (25) into Eq. (6) we obtain the following approximate expression for the polymer propagator

$$P(\mathbf{R}; n; \epsilon) = \int_0^{Z-1} dk \frac{\sin(kR) \sin[k\epsilon] [1 + (n-1)g_n] \frac{\sinh \frac{nq}{2} \frac{\epsilon}{k^2}}{k^2}}{2^2 R [1 + (n-1)g_n] \frac{\sinh \frac{nq}{2} \frac{\epsilon}{k^2}}{k^2}} : \quad (33)$$

In the limit of $\epsilon \rightarrow 0$, Eq. (33) becomes

$$P_{\text{Flexible}}(\mathbf{R}; n) = \frac{2(Z-1)^2}{R} \int_0^{Z-1} dk \frac{\sin(kR) [\sin k]^n}{k^{n+1}}; \quad (34)$$

which is the exact expression for the polymer propagator of the Random Flight Model[30]. Similarly, in the limit of $\epsilon \rightarrow 1$, we can perform the following expansion valid for large values of

$$\frac{\sinh \frac{nq}{2} \frac{\epsilon}{k^2}}{\frac{\sinh \frac{nq}{2} \frac{\epsilon}{k^2}}{k^2}} \sim \frac{\exp \frac{nq}{2} \frac{\epsilon}{k^2}}{\frac{\exp \frac{nq}{2} \frac{\epsilon}{k^2}}{k^2}} = \frac{\exp \frac{nq}{2} \frac{\epsilon}{k^2}}{k^2};$$

and compute the polymer propagator. The result is

$$P_{\text{rigid}}(\mathbf{R}; n; \epsilon) \sim \frac{2(Z-1)^2}{4Rn} \frac{\exp \frac{nq}{2} \frac{\epsilon}{k^2}}{k^2} (\mathbf{R} - n); \quad (35)$$

which is the polymer propagator of an infinitely stiff polymer chain[31]. This propagator is not normalized.

We now combine the approximate expression of the characteristic function, Eq. (25), with the Generalized Borel Transform to compute the polymer propagator and the single chain structure factor of the model.

We start the evaluation of the polymer propagator by rewriting Eq. (33) as follows

$$P(\mathbf{R}; n; \epsilon) = \frac{J(\mathbf{R}-1, (n-1)g_n; n; \epsilon) - J(\mathbf{R}+1, (n-1)g_n; n; \epsilon)}{4^2 R [1 + (n-1)g_n]}; \quad (36)$$

where $J(\mathbf{r}; n; \epsilon)$ is defined by the mathematical expression

$$J(\mathbf{r}; n; \epsilon) = \int_0^{Z-1} dk \frac{\sin[kr] \frac{\sinh \frac{nq}{2} \frac{\epsilon}{k^2}}{k^2}}{4 \cos[kr] \frac{\sinh \frac{nq}{2} \frac{\epsilon}{k^2}}{k^2}}; \quad (37)$$

This integral is evaluated exactly using GBT[21, 22, 23]. A brief summary of the GBT technique can be found in Appendix A.

We present the most important steps of the calculation hereafter and leave all the mathematical details for Appendix B. We first define an auxiliary function $G(b; n;)$ as follows

$$G(b; n;) = \int_0^{\infty} dw \exp(-wb) \frac{\sinh \frac{w}{2}}{w^2} \frac{1}{w^{2n}} \quad (38)$$

from which the function $J(x; n;)$ can be computed as the analytic continuation to the complex plane

$$J(x; n;) = \text{Re} f G(b = ix; n;) \quad (39)$$

Consequently, $J(x; n;)$ can be evaluated from the Laplace Transform given by Eq. (38).

Following the technique we can write

$$G(b; n;) = \lim_{N \rightarrow \infty} \left(\frac{1}{N!} \right)^N \int_0^{\infty} \frac{db}{b} \int_0^{\infty} \frac{dw}{w} \frac{(N+1)!}{b^{N+1}} \frac{\sinh \frac{w}{2}}{w^2} \frac{1}{w^{2n}} \quad (40)$$

The N integrations are computed using well-established properties and expansions of the functions $\sinh(x)$ and $[1 - x^2]$ [28]. After some straightforward algebra, we can write the analytical solution of $G(b; n;)$ for any even number of segments as follows

$$G(b; n;) = \sum_{k=0}^{\frac{n-2}{2}} \left(\frac{1}{k!} \right)^k \frac{1}{b^k} \frac{1}{(n-2k-1)!} \frac{[(n-2k-1)!]}{b^2} \quad (41)$$

where ${}_3F_2([k]; [k]; x)$ and $\Gamma(x)$ are the Generalized Hypergeometric[32] and Gamma[27] functions, respectively .

Replacing Eq.(41) into Eq.(39) and computing the analytic continuation to the complex plane through the substitution $b = ix$ we obtain

$$J(r; n;) = \frac{4}{2^n r} \sum_{k=0}^{\lfloor \frac{n-1}{2} \rfloor} \frac{(n-2k-1)!}{(2+n)!} \frac{r^k}{2^k} \frac{1}{k!} \frac{(n-2k-1)!}{r^2} \frac{1}{(2+n)!} \quad (42)$$

The imaginary part of the Generalized Hypergeometric function is calculated using its well-known analytical properties[32]. This function is an analytic function for values of the modulus of the argument z less than one and its continuation to the rest of complex plane generates a cut on the positive real axis starting at $\text{Re}(z) = 1$. This implies that only values of the argument, $\frac{[(n-2k-1)!]^2}{r^2}$, larger or equal to one will contribute to the imaginary part of ${}_3F_2(z)$. Consequently, this condition reduces the number of terms in the k sum such that the last term of Eq.(41) is $k = \frac{n-1}{2}$. The explicit evaluation of $\text{Im} \, {}_3F_2(z)$ can be found in Appendix C.

Finally, we replace Eq.(C15) into Eq.(42) to obtain the exact expression for $J(r; n;)$

$$J(r; n;) = \frac{1}{2^n} \sum_{k=0}^{\lfloor \frac{n-1}{2} \rfloor} \frac{(n-2k-1)!}{(2+n)!} \frac{r^k}{2^k} \frac{1}{k!} \frac{(n-2k-1)!}{r^2} \frac{1}{(2+n)!} \quad (43)$$

Note that Eq. (43) is just a sum of polynomials in r . The sum over the index k is the one obtained for the Random Flight Model[33] and imposes the finite extensibility of the polymer chain. The sums over the indexes n and L are a consequence of the stiffness of the polymer backbone. The expression of $J(r; n;)$ can be rewritten as follows

$$J(r; n;) = \frac{1}{2^n} \sum_{k=0}^{\lfloor \frac{n-1}{2} \rfloor} \frac{(n-2k-1)!}{(2+n)!} \frac{r^k}{2^k} \frac{1}{k!} \frac{(n-2k-1)!}{r^2} \frac{1}{(2+n)!} \quad (44)$$

which can be used for further approximation if so desired.

The expression for $J(r; n;)$ given by Eq. (43) was derived for even number of segments but, its validity for odd number of segments larger than two can be proved by analytic

continuation. Finally, in order to obtain the polymer propagator for semiflexible chains we have to replace Eq. (43) into Eq. (36). Observe that, after the replacement, Eq. (36) recovers the known exact solution of the Random Flight Model[33] when the limit $\kappa \rightarrow 0$ is taken. Indeed, the only term different from zero is the one for which $n = 0$.

Finally, we conclude our calculations of the WCM by computing the single chain structure factor which is defined by the following formula [29, 34]

$$S(\mathbf{k}; n) = \frac{1}{n+1} + \frac{2}{(n+1)^2} \sum_{n_i=1}^n \frac{(n-n_i+1)}{Z_{n_i}(\kappa)} K(\mathbf{k}; n_i) : \quad (45)$$

III. RESULTS AND DISCUSSION

Figures 1, 2 and 3 show the prediction of the normalized polymer propagator, Eq. (36), as function of the end-to-end distance for chains with 5, 10 and 30 Kuhn segments, and different values of the semiflexibility parameter κ . The numerical evaluation of the propagator was done using Eq. (43). The sum over the index n_i converges quickly even for large values of the semiflexibility parameter κ . Indeed, even with less than 80 terms in the sum we obtained a relative precision of 10^{-4} . The figures clearly show that the location of the peak in the polymer propagator (multiplied by R^2) moves toward larger values of R when the stiffness of the polymer backbone increases. This behavior is in good qualitative agreement with previous results arising from computer simulation studies[35] and theoretical approaches based on the Maximum Entropy Principle[20]. This is the correct result because the stiffer the polymer backbone, the higher the energetic penalty to bend the chain. Consequently, those configurations of the macromolecule with small end-to-end distance will be more and more hindered as the stiffness increases while those configurations with large end-to-end distance should be more and more favored. Therefore, the peak should shift toward larger values of R when the stiffness increases.

Figure 4 shows the polymer propagator for polymer chains with 5, 10 and 30 Kuhn segments and a fixed value of the semiflexibility parameter ($\kappa = 3.0$). This figure shows that the longer the polymer is, the more it behaves like a flexible chain since the location of peak (=end-to-end distance divided by the contour length) moves toward smaller values. In other words, the longer the polymer is, the less relevant the stiffness of the backbone becomes.

Figures 5, 6 and 7 show the behavior of $S(k; n; \epsilon)$, Eq. (45), as a function of k for different values of ϵ and three values of n (5, 10 and 30). The figures clearly show a decrease of the single chain structure factor with increasing k until it reaches a plateau at infinite k . Note that our computations predict that the decrease of the single chain structure factor for small values of k should be faster in the case of stiff polymers than in the case of flexible ones. This is a consequence of the fact that rigid polymers have a larger radius of gyration than flexible ones for a fixed chain length. In addition, the decrease of the structure factor for large values of k is faster for flexible polymers than for stiff ones. Indeed, our computations predict that the structure factor goes as k^{-d} for large values of k just before the plateau is reached. For values of $n=5, 10$ and 30 , the values of ϵ that we got were 1, 1.08 and 1.3 for $\epsilon=10$ (rigid) and 1.64, 1.9 and 2 for $\epsilon=0.33$ (flexible). These results are in good agreement with the fact that the structure factor of polymers with large chain length should scale as k^{-d} for large k values where d is the fractal dimension of the object (2 for a flexible polymer and 1 for a rigid polymer). Consequently, these results imply that for short polymer chains ($n = 5$), a value of $\epsilon = 10$ is high enough to make this polymer behave like stiff rod, k^{-1} . On the other hand, as the chain length increases we observe that $\epsilon = 10$ is not high enough to make the polymer behave as a rigid rod and deviations from the power law k^{-1} are observed. In the case of $\epsilon = 0.33$ our calculations predict that a value of n equal to five is not high enough to recover the scaling behavior of flexible chains, k^{-2} . But, as the number of segments increases, the exponent approaches the value of two, indicating that the polymer chain behaves more and more like a flexible one. This result was also showed in Figure 4. The figures also show that the approximation we developed in the previous section gives a smooth crossover behavior from the rigid to the flexible limit.

In order to make the presentation of our work more balanced and objective, we proceed to compare our results with the predictions of two other models. We start with our prediction for the single chain structure factor, $S(k)$, and compare it with the expression obtained by Kholodenko[17]. It has been shown that Kholodenko's result can describe experimental data quantitatively[19]. Thus, a comparison between our expression for the single chain structure factor and Kholodenko's will help us gauge the quality of the approximations used in our treatment of the WCM. Figures 8 and 9 show the comparison for polymers with $n = 30$ and two different values of the semiflexibility parameter (shown in the plots). We have

checked that other values of the parameters κ or a and n give quantitative agreements of similar quality. In all the cases studied we found that the relationship $\kappa = 2a$ always gives excellent quantitative agreement between the predictions of both models. Thus, our single chain structure factor should agree very well with the experimental data of Ballauff and coworkers. Still, since both models have different origins, some very small differences can be observed in the case of flexible chains (Figure 8).

We now proceed to compare our expression of the polymer propagator with the one computed by Wilhelm and Frey[11]. Figure 10 shows this comparison for the case of polymers with $n = 5$. The continuous curves are the results of our calculation with $\kappa = 1; 3; 5$ and 10. The dashed curves were constructed based on the work of Wilhelm and Frey where we adjusted the bending modulus such that the location of the peak in the propagator matched our results. This gives a better picture of the differences and similarities between both results. Figure 10 shows quantitative agreement between both results when the stiffness is low. As the stiffness increases Fig. 10 shows that the qualitative behavior of both propagators is still the same. For example, both results predict that the location of the peak moves toward larger values of the end-to-end distance and that the distribution becomes narrower. The main difference between both results is quantitative in nature. Our distribution becomes narrower than the one predicted by Wilhelm and Frey's work by a factor of two approximately which, in turn, generates a higher peak (the distributions are normalized).

Finally, let us conclude this section by rationalizing the origin of the discrepancy between the propagators and the reason why this does not affect the structure factor significantly. We first note that differences in the propagators are to be expected because both, ours and Frey's, calculations are based on different approximations and versions of the model (continuum or discrete). Let us now proceed to rationalize the origin of the discrepancy between both predictions. Equations (6) and (45) define the polymer propagator and single chain structure factor in terms of the characteristic function. Observe that the propagator is a Fourier transform of the characteristic function. Consequently, the oscillatory nature of the complex exponential generates partial cancellation of the contributions to the integral arising from different parts of the interval of integration. This cancellation magnifies any inaccuracies made in the approximation of the characteristic function. Moreover, the consequences of this cancellation become more and more important as the polymer becomes stiffer because

the characteristic function itself adopts an oscillatory behavior which, in principle, is out of phase with respect to the complex exponential. Therefore, the stiffer the polymer is, the more important the consequences of the approximation become. On the other hand, the evaluation of the structure factor from the characteristic function does not involve any oscillatory function. Consequently, any small inaccuracy made in the approximation of the characteristic function will remain small in the expression of the structure factor, as shown previously.

IV. CONCLUSIONS

The results obtained in this paper show that the Generalized Borel Transform is a very useful computational tool for the statistical mechanics of single semiflexible polymer chains. Indeed, the results presented in this paper clearly show that GBT is able to compute polymer propagators for single chain problems exactly. This capability of the technique is a direct consequence of its mathematical simplicity (the GBT requires elements of basic calculus and some fundamental knowledge of complex variables). Consequently, it does not add any mathematical complexity to the physics of the starting model.

Our analysis of the Wormlike Chain Model was based on an approximate expression of the characteristic function. The exact evaluation of this function is not possible at present. Therefore, we developed a new approximation that preserves the most relevant physical characteristics of the model intact. Specifically, our approach keeps the thermodynamics of the model, the flexible and rigid limits, the mean square end-to-end distance and the finite extensibility of the model intact while providing an approximate expression for the characteristic function for intermediate values of the stiffness of the polymer chain. The polymer propagator was obtained exactly from the approximate characteristic function using GBT. Note that the propagator is approximate not because of the GBT, which computes this quantity exactly, but because of the approximate nature of the characteristic function. Our expression for the propagator shows a peak that shifts toward larger values of the end-to-end distance as the stiffness of the polymer backbone is increased, in agreement with other theoretical and computational treatments of the model. We also found that, in the low wave vector region, the structure factor decreases faster with increasing wave

vector when the stiffness increases. This was rationalized in terms of the behavior of the radius of gyration. Similarly, we found that, in the large wave vector region, the structure factor of flexible chains decreases faster than the one of rigid polymers. This was compared with the behavior of very long polymer chains whose behavior for large wave vectors is known exactly. We also compared the predictions of our calculation with established results for the single chain structure factor and polymer propagator. Excellent quantitative agreement was observed between our prediction for the single chain structure factor and the one predicted by Kholodenko's model. The polymer propagator was compared with the prediction of Wilhelm and Frey. Very good quantitative agreement was observed between the predictions of both models for low values of the stiffness. For stiff polymers, quantitative deviations were observed and the origin of the deviations was rationalized.

The proposed approach to semiflexible polymers can also address semiflexible polymers with other topologies like ring and m-arm star polymers. The procedure should be similar to the one presented in this paper but, the characteristic function will have a different mathematical expression.

We conclude this section with a discussion of the characteristic function of the WCM which limits our ability to solve this model exactly. Let us rewrite this function. The expression is

$$K(\mathbf{k}; g; n; l) = \int d\mathbf{R}_k g^n (\mathbf{R}_j - \mathbf{l}) \exp^{i \sum_{j=1}^n \mathbf{R}_j \cdot \mathbf{k}} + \sum_{i=1}^{n-1} \mathbf{R}_{i+1} \cdot \mathbf{k} \quad (46)$$

where we have replaced the wave vector \mathbf{k} by a group of wave vectors \mathbf{k}_j . This expression is the one of the characteristic function when all the \mathbf{k}_j are equal to \mathbf{k} . Observe that if we replace \mathbf{k}_j by $i\mathbf{b}_j$ where i is the imaginary unit, then

$$K(i\mathbf{b}; g; n; l) = \int d\mathbf{R}_k g^n (\mathbf{R}_j - \mathbf{l}) \exp^{\sum_{j=1}^n \mathbf{R}_j \cdot \mathbf{b}} + \sum_{i=1}^{n-1} \mathbf{R}_{i+1} \cdot \mathbf{b} \quad (47)$$

which has the form of a Laplace Transform in $3n$ dimensions. But, the GBT computes Laplace Transforms very accurately or even exactly. Consequently, a generalization of GBT to many dimensions might lead to an exact or very accurate expression of the characteristic function of the WCM. This expression can be further used to compute the polymer propagator using GBT. Thus, we speculate that such extension of the GBT technique might allow

us to solve very accurately or even exactly the Wormlike Chain Model. In general, such extension of GBT might allow us to solve other models of polymer chains of the form

$$K(\mathbf{f}; \mathbf{g}; n; \text{parameters}) = \int_0^Z d\mathbf{f} \int_{\mathbf{R}_j}^{\mathbf{X}^n} \exp(-i \mathbf{f} \cdot \mathbf{R}_j) \int_0^1 d\mathbf{R}_1 \exp(i \mathbf{f} \cdot \mathbf{R}_1) \exp(-H[\mathbf{R}_1; \mathbf{g}; \text{parameters}]); \quad (48)$$

where $H[\mathbf{R}_1; \mathbf{g}; \text{parameters}]$ is the Hamiltonian of the model. Thus, helical wormlike polymers and other models might be mathematically tractable with this generalization of the GBT.

V. ACKNOWLEDGMENTS

We acknowledge the National Science Foundation, Grant # CHE-0132278 (CAREER), the Ohio Board of Regents Action Fund, Proposal # R566 and The University of Akron for financial support.

Appendix A: THE GENERALIZED BOREL TRANSFORM (GBT)

Let us briefly present the mathematical aspects of the GBT in connection with the computation of the Laplace-Mellin transform[21, 22, 23]. We start with the expression

$$S(\mathbf{g}; \mathbf{a}; n) = \int_0^Z \mathbf{x}^n H(\mathbf{x}; \mathbf{a}) \exp(-\mathbf{g} \cdot \mathbf{x}) d\mathbf{x}; \quad \mathbf{g} > 0 \quad (A1)$$

where we have explicitly extracted a factor \mathbf{x}^n from the function to be transformed.

Defining the Generalized Borel Transform (GBT) of S as

$$B(s; \mathbf{a}; n) = \int_0^Z \exp[s \cdot \mathbf{x}] \frac{1}{1 + \exp(-\mathbf{g} \cdot \mathbf{x})} S(\mathbf{g}; \mathbf{a}; n) d\mathbf{x}; \quad \text{Re}(s) < 0 \quad (A2)$$

where \mathbf{g} is any real positive non-zero value and $1 = \exp(-\mathbf{g} \cdot \mathbf{x})$, we can invert Eq. (A2) in the following way

$$S(\mathbf{g}; \mathbf{a}; n) = 2^{-2} (1 - \exp(-\mathbf{g} \cdot \mathbf{x})) \int_0^Z \int_0^Z \exp[G(\mathbf{w}; \mathbf{t}; \mathbf{g}; \mathbf{a}; n)] d\mathbf{w} d\mathbf{t}; \quad (A3)$$

where the explicit expression of $G(\mathbf{w}; \mathbf{t}; \mathbf{g}; \mathbf{a}; n)$ is not important for our present purposes (for more details see Ref. [22]).

The expression given by Eq. (A3) is valid for any non-zero, real and positive value of the parameter β . But, the resulting expression for $S(\mathbf{g}; \mathbf{a}; n)$ does not depend on β explicitly. Thus, we can choose the value of this parameter in such a way that it allows us to solve Eq. (A3). The dominant contribution to the double integral is obtained using steepest descent [36, 37] in the combined variables $[\mathbf{t}; \mathbf{w}]$. In doing so, one first computes the saddle point $\mathbf{t}_o(\mathbf{g}; \mathbf{a}; n)$ and $\mathbf{w}_o(\mathbf{g}; \mathbf{a}; n)$ in the limit $\beta \rightarrow 1$ and then checks the positivity condition [38] (the Hessian of G at this point should be positive) obtaining

$$\mathbf{t}_o = \ln \frac{\mathbf{x}_o^2(\mathbf{g}; \mathbf{a}; n)}{f(\mathbf{x}_o(\mathbf{g}; \mathbf{a}; n); \mathbf{a}; n)} = \mathbf{t}_o(\mathbf{g}; \mathbf{a}; n) \quad ; \quad \mathbf{w}_o = \ln [\mathbf{x}_o(\mathbf{g}; \mathbf{a}; n)] = \mathbf{w}_o(\mathbf{g}; \mathbf{a}; n); \quad (\text{A4})$$

where $\mathbf{x}_o(\mathbf{g}; \mathbf{a}; n)$ is the real and positive solution of the implicit equation coming from the extremes of the function G in the asymptotic limit in β . Therefore, one obtains the following equation

$$\mathbf{x}_o^2 g^2 = f(\mathbf{x}_o; \mathbf{a}; n) [f(\mathbf{x}_o; \mathbf{a}; n) + 1]; \quad (\text{A5})$$

where

$$f(\mathbf{x}_o; \mathbf{a}; n) = 1 + n + \mathbf{x}_o \frac{d \ln [H(\mathbf{x}_o; \mathbf{a})]}{d \mathbf{x}_o}; \quad (\text{A6})$$

In the range of the parameters where $f(\mathbf{x}_o; \mathbf{a}; n) > 1$ which is fulfilled when $n > 1$, and assuming that there is only one saddle point, we can retain the first order in the expansion of G around the saddle point.

Finally, we obtain the approximate expression for the starting function $S(\mathbf{g}; \mathbf{a}; n)$

$$S_{\text{Aprox}}(\mathbf{g}; \mathbf{a}; n) = \frac{1}{2} e^{-\frac{1}{2} \frac{f(\mathbf{x}_o; \mathbf{a}; n) + 1}{D(\mathbf{x}_o; \mathbf{a}; n)}} [\mathbf{x}_o]^{n+1} H(\mathbf{x}_o; \mathbf{a}) \exp[-f(\mathbf{x}_o; \mathbf{a}; n)]; \quad (\text{A7})$$

where

$$D(\mathbf{x}_o; \mathbf{a}; n) = \mathbf{x}_o \frac{df(\mathbf{x}_o; \mathbf{a}; n)}{d \mathbf{x}_o} [1 + 2 + f(\mathbf{x}_o; \mathbf{a}; n)] + f(\mathbf{x}_o; \mathbf{a}; n) [1 + f(\mathbf{x}_o; \mathbf{a}; n)]; \quad (\text{A8})$$

Note that the expression given by Eq. (A7) is valid for functions $H(\mathbf{x}; \mathbf{a})$ that fulfill the following general conditions:

- 1) the relation given by Eq. (A5) must be biunivocal.

- 2) $D(\mathbf{x}_o; \mathbf{a}; n)$ has to be positive and $\mathbf{x}_o \frac{dD(\mathbf{x}_o; \mathbf{a}; n)}{d\mathbf{x}_o} - 2f(\mathbf{x}_o; \mathbf{a}; n)$ has to be negative in \mathbf{x}_o .
- 3) $f(\mathbf{x}_o; \mathbf{a}; n) = 1$. In particular, this condition is fulfilled when $n = 1$:

These conditions provide the range of values of the parameters where the approximate solution, Eq. (A7), is valid.

In summary, the GBT provides an approximate solution, Eq. (A7), to amplitudes with the mathematical form given by Eq. (A1). The calculation consists of solving the implicit equation Eq. (A5) for $n = 1$ to obtain the saddle point and replace it into Eq. (A7).

Let us now focus on amplitudes with the mathematical form of a Laplace transform

$$S(\mathbf{g}; \mathbf{a}) = \int_0^Z H(\mathbf{x}; \mathbf{a}) \exp(-\mathbf{g}\mathbf{x}) d\mathbf{x} \quad \mathbf{g} > 0: \quad (\text{A9})$$

This kind of amplitudes can be mapped onto expressions of the form given by Eq. (A1). In order to use the GBT on Eq. (A9), we use the following relationship between Eq. (A9) and Eq. (A1)

$$S(\mathbf{g}; \mathbf{a}; n) = \left(\int \right)^n \frac{d^n}{d\mathbf{g}^n} S(\mathbf{g}; \mathbf{a}); \quad (\text{A10})$$

which can be inverted to give

$$S(\mathbf{g}; \mathbf{a}) = \left(\int \right)^n \frac{d^n}{d\mathbf{g}^n} S(\mathbf{g}; \mathbf{a}; n) + \sum_{p=0}^{n-1} c_p(\mathbf{a}; n) \mathbf{g}^p: \quad (\text{A11})$$

The finite sum comes from the indefinite integrations. Note that all the coefficients vanish whenever the Laplace transform, Eq. (A9), fulfills the following asymptotic behavior

$$\lim_{g \rightarrow 1} S(\mathbf{g}; \mathbf{a}) = 0: \quad (\text{A12})$$

In addition, the expression, given by Eq. (A11), is valid for any value of n ; in particular for $n = 1$: Consequently, if Eq. (A12), is fulfilled, then the analytical solution reads

$$S(\mathbf{g}; \mathbf{a}) = \lim_{n \rightarrow 1} \left(\int \right)^n \frac{d^n}{d\mathbf{g}^n} S_{\text{Aprox}}(\mathbf{g}; \mathbf{a}; n); \quad (\text{A13})$$

where, for $n = 1$, we can use the expression given by Eq. (A7). It is important to note that it is the limit $n \rightarrow 1$ that makes the saddle point solution, Eq. (A7), an exact solution for

Eq. (A3). Thus, as long as the n indefinite integrals can be done without approximations, as it is in our case, the result for S is exact.

Appendix B: EVALUATION OF THE POLYMER PROPAGATOR

We start the evaluation of the polymer propagator by rewriting Eq. (38) as follows

$$G(\mathbf{b}; n; \mathbf{c}) = \frac{\partial^{n-1}}{\partial \mathbf{c}^{n-1}} \int_0^Z dw \exp(-w\mathbf{b}) \exp\left\{ \frac{\sinh\left(\frac{nq}{2} \frac{w^2}{w^2 + 2}\right)}{2} \right\} \mathbf{A} \mathbf{c} \quad (B1)$$

$$= \frac{\partial^{n-1}}{\partial \mathbf{c}^{n-1}} f G_A(\mathbf{b}; \mathbf{c}) g_{\mathbf{c}=0} \mathbf{c}$$

where $G_A(\mathbf{b}; \mathbf{c})$ is

$$G_A(\mathbf{b}; \mathbf{c}) = \int_0^Z dw \exp(-w\mathbf{b}) H(\mathbf{w}; \mathbf{c}) \quad (B2)$$

and $H(\mathbf{w}; \mathbf{c})$ is given by the expression

$$H(\mathbf{w}; \mathbf{c}) = \exp\left\{ \frac{\sinh\left(\frac{nq}{2} \frac{w^2}{w^2 + 2}\right)}{2} \right\} \mathbf{A} \mathbf{c} \quad (B3)$$

The integral expressed by Eq.(B2) satisfies all the requirements of the GBT technique. Then, we evaluate it in the following way

$$G_A(\mathbf{b}; \mathbf{c}) = \lim_{N \rightarrow \infty} \left(\frac{1}{N} \int_0^Z dw \exp(-w\mathbf{b}) H(\mathbf{w}; \mathbf{c}) \right) \quad (B4)$$

where

$$G_{A_N}(\mathbf{b}; \mathbf{c}) = \int_0^Z dw w^N \exp(-w\mathbf{b}) H(\mathbf{w}; \mathbf{c}) \quad (B5)$$

In the asymptotic limit of $N \rightarrow \infty$ the GBT provides an analytical solution for Eq.(B5). Following the technique, we solve the implicit equation, Eq. (A5), for the saddle point w_0 . The asymptotic solution is

$$w_0 = \frac{N + 3/2}{b} \quad (B6)$$

Replacing this expression for w_0 in the expression provided by the GBT, Eq. (A7), we obtain

$$G A_N(b; c) = \frac{(N+1)!}{b^{N+1}} H_{\frac{N+3}{2}} \left(\frac{c}{b} \right); c \rightarrow 0 \quad (B7)$$

Furthermore, we replace Eq.(B7) into Eq.(B4) and the resulting expression into Eq.(B1), and we exchange the order of the operators in the resulting expression. In other words, we first evaluate the n derivatives with respect to c and, afterward, we take the limit of $c \rightarrow 0$ to obtain the expression given by Eq. (40). Next, we solve the N integrations using standard properties and expansions of the functions $\sin(x)$ and $[1-x^2]$ [28], and write $G(b; n)$ as follows

$$G(b; n) = \frac{1}{2^{n/2}} \sum_{k=0}^{\frac{n-2}{2}} \binom{n-2}{2k} \frac{1}{b^k} M(N; n; k; b); \quad (B8)$$

where n is even and

$$M(N; k; b) = \lim_{N \rightarrow \infty} \frac{1}{N!} \int_0^1 dx \frac{(i(n-1-2k))^N}{r!} \frac{1}{b^{2+N-n+r/2}}; \quad (B9)$$

where $L(x)$ are the Laguerre polynomials [28].

Note that the only powers on b in Eq. (B9) that fulfill the asymptotic behavior of the function $G(b; n)$ are those for which the condition $r = (n+2-1)$ is satisfied. Therefore, the N indefinite integrations are exactly doable. The result is

$$\int_0^1 dx \frac{1}{b^{2+N-n+r/2}} = \frac{(2+r-n/2)}{(2+N-n+r/2)} \frac{(1)^N}{b^{2+r-n/2}}; \quad (B10)$$

Replacing Eq. (B10) into Eq. (B9) and after the change of variables $r = x+2+n-1$; we can write

$$M(N; k; b) = \int_0^1 dx \frac{1}{b} \frac{(i(n-2k-1))^{N-n-1}}{b^{2+N-n+r/2}} \frac{(1)^N}{b^{2+r-n/2}}; \quad (B11)$$

Using the asymptotic properties of the Gamma function[27]

$$\lim_{N \rightarrow \infty} \frac{N^x (N+1)}{(N+x+1)} = 1; \quad (\text{B12})$$

Eq. (B11) finally reads

$$M(n; k; ; b) = \frac{1}{b} \text{Im}_{x=0} \sum_{x=0}^{\infty} (i(n-2k-1))^2 + n-1 \frac{(n-2)^2}{x!} \frac{i(n-2k-1)^2}{b} \frac{x!}{(x+1) \frac{x+2}{2} + \frac{x+2}{2}} \quad (\text{B13})$$

The sum over x is exactly doable. The result is

$$M(n; k; ; b) = \frac{1}{b} \text{Im}_{x=0} \sum_{x=0}^{\infty} (i(n-2k-1))^2 + n-1 \frac{(n-2)^2}{x!} F D (; n; k; b); \quad (\text{B14})$$

where

$$F D (; n; k; b) = \frac{(n+1) {}_3F_2 \left(1; \frac{1}{2}; +1; +1; +\frac{n+1}{2}; +\frac{n}{2}; \frac{[(n-2k-1)^2]_n}{b^2} \right)}{(2+n+1)} + \frac{2i(n-2k-1)^2}{b} \frac{{}_3F_2 \left(\frac{3}{2}; 1; 1; +\frac{n}{2}+1; +\frac{n}{2}+\frac{1}{2}; \frac{[(n-2k-1)^2]_n}{b^2} \right)}{(2+n+1)} : \quad (\text{B15})$$

Equation (B14) clearly shows that the imaginary part affects only the real part of the function $F D (; n; k; b)$. Thus, the final expression for $G(b; n;)$ is given by Eq. (41).

Appendix C: EVALUATION OF THE IMAGINARY PART OF THE GENERALIZED HYPERGEOMETRIC FUNCTION

We evaluate $\text{Im} \, {}_3F_2(z)$ using the following integral representation of the Hypergeometric function[28]

$${}_3F_2 \left(1; \frac{1}{2}; +1; +1; +\frac{n+1}{2}; +\frac{n}{2}; \frac{[(n-2k-1)^2]_n}{b^2} \right) = \frac{b^{2(n+1)}}{B(1; 2+n-1)} \frac{1}{(n-2k-1)^2 + n-1} \int_0^1 \frac{dx}{x^2 + b^2} \quad (\text{C1})$$

which is valid for values of n equal or larger than two. The analytic continuation to the complex plane is done as before through the replacement $b = -ir$. Then, the imaginary part of the Hypergeometric function is

$$\begin{aligned} \text{Im} \left({}_3F_2 \left(1; \frac{1}{2}, \frac{1}{2} + 1; -\frac{n+1}{2}, -\frac{n}{2}; \frac{(n-2k-1)!}{r^2} \right) \right) = \\ \frac{r^{2(n+1)} ()^{+1}}{\Gamma(n-2k-1) \Gamma(n-2k-1) \Gamma(n-2k-1) \Gamma(n-2k-1) \Gamma(n-2k-1)} \\ \text{Im} \int_0^{\frac{1}{r}} \frac{B(1; 2+n-1) (n-2k-1)!^{n-1}}{[n-2k-1] \frac{1}{x^{n-2}} x^2 \frac{1}{r^{n-1}}} dx: \end{aligned} \quad (C2)$$

Thus, we have to evaluate the expression

$$L = \text{Im} \int_0^{\frac{1}{r}} \frac{B(1; 2+n-1) (n-2k-1)!^{n-1}}{[n-2k-1] \frac{1}{x^{n-2}} x^2 \frac{1}{r^{n-1}}} dx: \quad (C3)$$

After analyzing the analytical behavior of the integrand we concluded that we can exchange the operations of integration and imaginary part to obtain

$$L = \int_0^{\frac{1}{r}} \frac{B(1; 2+n-1) (n-2k-1)!^{n-1}}{[n-2k-1] \frac{1}{x^{n-2}} x^2 \frac{1}{r^{n-1}}} \text{Im} \frac{1}{(x-r)^{+1}} dx: \quad (C4)$$

Thus, we have to compute

$$LS = \text{Im} \left(\frac{1}{(x-r)^{+1}} \right); \quad (C5)$$

first and, afterward, we have to solve the integral given by Eq. (C4).

The analytical behavior of the function $(x-r)^{-1}$ is well known[28]. It is an analytic function for $|x| > R$ but, its analytic continuation to the complex plane generates a cut on the real axis in the range $-R < \text{Re}(x) < R$ which provides its imaginary part. Writing

$$\frac{1}{(x-R)^{+1}} = \frac{1}{(x-R)} \mathcal{P} \frac{1}{x-R} \quad (C6)$$

for integer values of n and $x > R$, and using the following integral representation

$$\mathcal{P} \frac{1}{x-R} = \int_0^1 dy \exp \left(-\frac{y}{x-R} \right); \quad (C7)$$

valid for $x > R$, we obtain the result

$$\text{Im} \left(\frac{1}{(x-R)^{+1}} \right) = \frac{()^{+1}}{(R-x)} \text{Re} \int_0^1 du \exp \left[-\frac{u}{(R-x)} \right]; \quad (C8)$$

where $\mathbf{x} < R$.

Using parity's properties of the function $\cos(\cdot)$; we extend the range of the integration in Eq. (C8) to obtain

$$\text{Im} \left(\frac{1}{(\mathbf{x} - R)^{+1}} \right) = \frac{1}{(\mathbf{x} - R)} (\mathbf{x} - R) = \frac{(\cdot)}{!} \frac{\partial}{\partial (\mathbf{x} - R)} (\mathbf{x} - R) : \quad (\text{C9})$$

Finally, we replace the expression given by Eq. (C9) into Eq. (C4) and perform the change of variables $\mathbf{y} = \mathbf{x} - \mathbf{r}$ to obtain

$$L = \frac{(\cdot)}{!} \int_{\mathbf{r}}^{\mathbf{z} - \mathbf{n} - 2\mathbf{k} - 1 - \mathbf{r}} F_k(\mathbf{y}; \mathbf{n}; \mathbf{r}) \frac{\partial}{\partial \mathbf{y}} (\mathbf{y}) d\mathbf{y}; \quad (\text{C10})$$

where $F_k(\mathbf{y}; \mathbf{n}; \mathbf{r})$ is defined as

$$F_k(\mathbf{y}; \mathbf{n}; \mathbf{r}) = \int_{\mathbf{n} - 2\mathbf{k} - 1 - \mathbf{r}}^{\mathbf{z} - \mathbf{n} - 2\mathbf{k} - 1 - \mathbf{r}} [\mathbf{y} + 2\mathbf{r}]^{-1} : \quad (\text{C11})$$

Integrating by parts times, we obtain the following final expression

$$L = - \frac{(\cdot)}{!} \left(\frac{\partial F_k(\mathbf{y}; \mathbf{n}; \mathbf{r})}{\partial \mathbf{y}} \right)_{\mathbf{y}=0} : \quad (\text{C12})$$

The derivatives are computed as follows

$$\left(\frac{\partial F_k(\mathbf{y}; \mathbf{n}; \mathbf{r})}{\partial \mathbf{y}} \right)_{\mathbf{y}=0} = \sum_{L=0}^{\infty} \frac{(\cdot)}{!} \left(\frac{\partial^L}{\partial \mathbf{y}^L} \int_{\mathbf{n} - 2\mathbf{k} - 1 - \mathbf{r}}^{\mathbf{z} - \mathbf{n} - 2\mathbf{k} - 1 - \mathbf{r}} [\mathbf{y} + 2\mathbf{r}]^{-1} d\mathbf{y} \right)_{\mathbf{y}=0} ; \quad (\text{C13})$$

to obtain

$$\left(\frac{\partial F_k(\mathbf{y}; \mathbf{n}; \mathbf{r})}{\partial \mathbf{y}} \right)_{\mathbf{y}=0} = \sum_{L=0}^{\infty} \frac{(\cdot)}{!} \frac{(2 - L)!(2 + \mathbf{n} - 2)! \int_{\mathbf{n} - 2\mathbf{k} - 1 - \mathbf{r}}^{\mathbf{z} - \mathbf{n} - 2\mathbf{k} - 1 - \mathbf{r}} [\mathbf{y} + 2\mathbf{r}]^{-1} d\mathbf{y}}{(2 + \mathbf{n} - 2 - L)!(\cdot)!(2\mathbf{r})^{2 + 1 - L}} : \quad (\text{C14})$$

Finally, we replace Eq. (C14) into Eq. (C12) and the resulting expression into Eq. (C2) to obtain the final expression of $\text{Im } f_3 F_2 g$

$$\text{Im } f_3 F_2 g = \frac{(2+n)}{(n-2k-1)^{2+n-1} [(n+1)]^2} \times \frac{B_0}{B_1} \frac{C_A}{C_L} \frac{(2-L)!}{(2)^{2+1-L}} \quad (C15)$$

$$\frac{r^L [n-2k-r-1]^{n-2-L}}{(2+n-2-L)!} \quad n-2:$$

- [1] M. G. Poirier *et al.*, *Phys. Rev. Lett.* **86**, **360** (2001); J. F. Leger *et al.*, *Phys. Rev. Lett.* **83**, 1066 (1999); V. Parpura and J. M. Fernandez, *Biophys. J.* **71**, 2356 (1996); M. D. Wang *et al.*, *Biophys. J.* **72**, 1335 (1997); A. D. Mehta, K. A. Pullen and A. Spudich, *FEBS Lett.* **430**, 23 (1998); A. D. Mehta, M. Rief and J. A. Spudich, *J. Biol. Chem.* **274**, 14517 (1999); T. E. Fisher, P. E. Marszalek and J. M. Fernandez, *Nat. Struct. Biol.* **7**, 719 (2000); T. E. Fisher *et al.*, *Trends Biochem. Sci.* **24**, 379 (1999); M. Carrion-Vazquez *et al.*, *Prog. Biophys. Mol. Biol.* **74**, 63 (2000); T. T. Perkins, S. R. Quake, D. E. Smith and S. Chu, *Science* **264**, 822 (1994); S. B. Smith, Y. Cui and C. Bustamante, *Science* **271**, 795 (1996); T. T. Perkins, D. E. Smith and S. Chu, *Science* **276**, 2016 (1997); A. F. Oberhauser, P. E. Marszalek, H. P. Erickson and J. M. Fernandez, *Nature (London)* **393**, 181 (1998); F. Oesterhelt, M. Rief and H. E. Gaub, *New J. Phys.* **1**, 6.1 (1999); H. B. Li, W. K. Zhang, W. Q. Xu and X. Zhang, *Macromolecules* **33**, 465 (2000).
- [2] J. F. Marko and E. D. Siggia, *Macromolecules* **28**, 8759 (1995); K. Kroy and E. Frey, *Phys. Rev. Lett.* **77**, 306 (1996).
- [3] G. Porod, *Monatsh. Chem.* **80**, 251 (1949); O. Kratky and G. Porod, *Rec. Trav. Chim.* **68**, 1106 (1949).
- [4] L. Eichinger *et al.*, *Biophys. J.* **70**, 1054 (1996); P. Janmey *Cell Membranes and the Cytoskeleton*, Vol. 1A of *Handbook of Biological Physics*, chapter 17, page 805 (North Holland, Amsterdam, 1995); P. A. Janmey, *Curr. Op. Cell. Biol.* **2**, 4 (1991).
- [5] N. Saito, K. Takahashi and Y. Yunoki, *Journal of the Physical Society of Japan*, **22**, 219 (1967).
- [6] H. Yamakawa, *Helical Worm-like Chains in Polymer Solutions* (Springer, Berlin, 1997).
- [7] M. Fixman and J. Kovac, *J. Chem. Phys.* **58**, 1564 (1973).
- [8] R. A. Harris and J. E. Hearst, *J. Chem. Phys.* **44**, 2595 (1966).
- [9] H. E. Daniels, *Proc. Roy. Soc. Edinburgh* **A63**, 290 (1952); W. Gobush, H. Yamakawa, W. H.

- Stockmayer and W. S. Magee, *J. Chem. Phys.* **57**, 2839 (1972).
- [10] H. Yamakawa, *Pure and Appl. Chem.* **46**, 135 (1976).
- [11] J. Wilhelm and E. Frey, *Phys. Rev. Lett.* **77**, 2581 (1996); P. L. Hansen and R. Podgornik, *J. Chem. Phys.* **114**, 8637 (2001).
- [12] M. G. Bawendi and K. F. Freed, *J. Chem. Phys.* **83**, 2491 (1985); J. B. Lagowski, J. Noolandi and B. Nickel, *J. Chem. Phys.* **95**, 1266 (1991); G. A. Carri and M. Muthukumar, *J. Chem. Phys.* **109**, 11117 (1998).
- [13] R. G. Winkler, P. Reineker and L. Harnau, *J. Chem. Phys.* **101**, 8119 (1994).
- [14] C. M. Marques and G. H. Fredrickson, *J. Phys. II France* **7**, 1805 (1997).
- [15] L. Harnau, R. G. Winkler and P. Reineker, *J. Chem. Phys.* **104**, 6355 (1996); K. Kroy and E. Frey, *Phys. Rev. E* **55**, 3092 (1997).
- [16] A. L. Kholodenko, *Ann. Phys.* **202**, 186 (1990); A. L. Kholodenko *J. Chem. Soc. Faraday Trans.* **91**, 2473 (1995); A. L. Kholodenko, *Phys. Lett. A* **141**, 351 (1989); A. L. Kholodenko, *Phys. Lett. A* **178**, 180 (1993); A. Kholodenko and T. Vilgis *Phys. Rev. E* **50**, 1257 (1994), A. L. Kholodenko and T. A. Vilgis *Phys. Rev. E* **52**, 3973 (1995).
- [17] A. L. Kholodenko, *Macromolecules* **26**, 4179 (1993).
- [18] A. Kholodenko, M. Ballauff and M. Aguero Granados, *Physica A* **260**, 267 (1998).
- [19] M. Ballauff *et al.*, *Macromolecules* **30**, 273 (1997).
- [20] R. G. Winkler, *J. Chem. Phys.* **118**, 2919 (2003).
- [21] L.N.Epele, H. Fanchiotti, C.A. Garcia Canal and M. Marucho, *Phys. Lett.* **B523**, 102 (2001).
- [22] L.N.Epele, H. Fanchiotti, C.A. Garcia Canal and M. Marucho, *Phys. Lett.* **B556**, 87 (2003).
- [23] L.N.Epele, H. Fanchiotti, C.A. Garcia Canal and M. Marucho, *Nucl. Phys.* **B583**, 454 (2000).
- [24] S. M. Bhattacharjee and M. Muthukumar, *J. Chem. Phys.* **86**, 411(1987).
- [25] K. F. Freed in *Advances in Chemical Physics*, Vol. 22, Pages 1-128, I. Prigogine and Stuart A. Rice Editors (John Wiley and Sons, New York, 1972).
- [26] G. Arfken, *Mathematical Methods for Physicists* (Academic Press, Inc., New York, 1985).
- [27] M. Abramowitz and I. Stegun, *Handbook of Mathematical Functions* (Dover, New York, 1970).
- [28] I.S. Gradshteyn and I.M. Ryzhik, *Table of Integrals, Series, and Products* (Academic Press, New York, 2000).
- [29] H. Benoit and P. Doty, *J. Phys. Chem.* **57**, 958 (1953).

- [30] K. F. Freed, *Renormalization Group Theory of Macromolecules* (John Wiley & Sons, New York, 1987).
- [31] P. G. de Gennes, *Biopolymers* **6**, 715 (1968).
- [32] H. Bateman, *Higher Transcendental Functions* (Mc Graw Hill, New York, 1953).
- [33] M. C. Wang and E. Guth, *J. Chem. Phys.* **20**, 1144 (1952); C. Hsiung, H. Hsiung and A. Gordus, *J. Chem. Phys.* **34**, 535 (1961).
- [34] W. L. Mattice and U. W. Suter, *Conformational Theory of Large Macromolecules: The Rotational Isomeric State Model in Macromolecular Systems* (John Wiley & Sons, New York, 1994).
- [35] J. Wilhelm and E. Frey, *Phys. Rev. Lett.* **77**, 2581 (1996).
- [36] N. Bleistein and R. Handelsman, *Asymptotic Expansion of Integrals* (Dover, New York, 1986).
- [37] E. T. Copson, *Asymptotic Expansions* (Cambridge University Press, 1965).
- [38] H. Jeffrey and B. S. Jeffrey, *Methods of Mathematical Physics* (Cambridge University Press, 1966).

List of Figures

FIG. 1: Normalized polymer propagator $4 R^{-2} P(R; n; \epsilon) = Z_n(\epsilon)$ versus R/n for $n = 5$. Continuous line ($\epsilon = 0.33$), dotted line ($\epsilon = 1.0$), dashed line ($\epsilon = 3.0$), long dashed line ($\epsilon = 5.0$) and dashed-dotted line ($\epsilon = 10.0$).

FIG. 2: Normalized polymer propagator $4 R^{-2} P(R; n; \epsilon) = Z_n(\epsilon)$ versus R/n for $n = 10$. Continuous line ($\epsilon = 0.33$), dotted line ($\epsilon = 1.0$), dashed line ($\epsilon = 3.0$), long dashed line ($\epsilon = 5.0$) and dashed-dotted line ($\epsilon = 10.0$).

FIG. 3: Normalized polymer propagator $4 R^{-2} P(R; n; \epsilon) = Z_n(\epsilon)$ versus R/n for $n = 30$. Continuous line ($\epsilon = 0.33$), dotted line ($\epsilon = 1.0$), dashed line ($\epsilon = 3.0$), long dashed line ($\epsilon = 5.0$) and dashed-dotted line ($\epsilon = 10.0$).

FIG. 4: Normalized polymer propagator $4 R^{-2} P(R; n; \epsilon) = Z_n(\epsilon)$ versus R/n for $\epsilon = 3.0$. Continuous line ($n = 30$), dashed line ($n = 10$) and dashed-dotted line ($n = 5$).

FIG. 5: Single chain structure factor $S(k; n; \epsilon)$ versus wave vector k for $n = 5$. Continuous line ($\epsilon = 0.33$), dotted line ($\epsilon = 1.0$), dashed line ($\epsilon = 3.0$), dashed-dotted line ($\epsilon = 10.0$) and circles (best fits to the power law in the range $k \in (2; 3)$ for $\epsilon = 0.33$ and $\epsilon = 10.0$).

FIG. 6: Single chain structure factor $S(k; n; \epsilon)$ versus wave vector k for $n = 10$. Continuous line ($\epsilon = 0.33$), dotted line ($\epsilon = 1.0$), dashed line ($\epsilon = 3.0$), dashed-dotted line ($\epsilon = 10.0$) and circles (best fits to the power law in the range $k \in (2; 3)$ for $\epsilon = 0.33$ and $\epsilon = 10.0$).

FIG. 7: Single chain structure factor $S(k; n; \epsilon)$ versus wave vector k for $n = 30$. Continuous line ($\epsilon = 0.33$), dotted line ($\epsilon = 1.0$), dashed line ($\epsilon = 3.0$), dashed-dotted line ($\epsilon = 10.0$) and circles (best fits to the power law in the range $k \in (2; 3)$ for $\epsilon = 0.33$ and $\epsilon = 10.0$).

FIG. 8: Single chain structure factor $S(k; n; \epsilon)$ versus wave vector k for $n = 30$. (Line) Kholodenko's model with $a = 1$, (points) this work with $\epsilon = 2$.

FIG. 9: Single chain structure factor $S(k; n; \epsilon)$ versus wave vector k for $n = 30$. (Line) Kholodenko's model with $a = 50$, (points) this work with $\epsilon = 100$.

FIG. 10: Normalized polymer propagator $P(R;n)$ versus end-to-end distance R in units of Kuhn length for $n = 5$. (Continuous lines) this work, (dashed lines) Wilhelm and Frey's results.

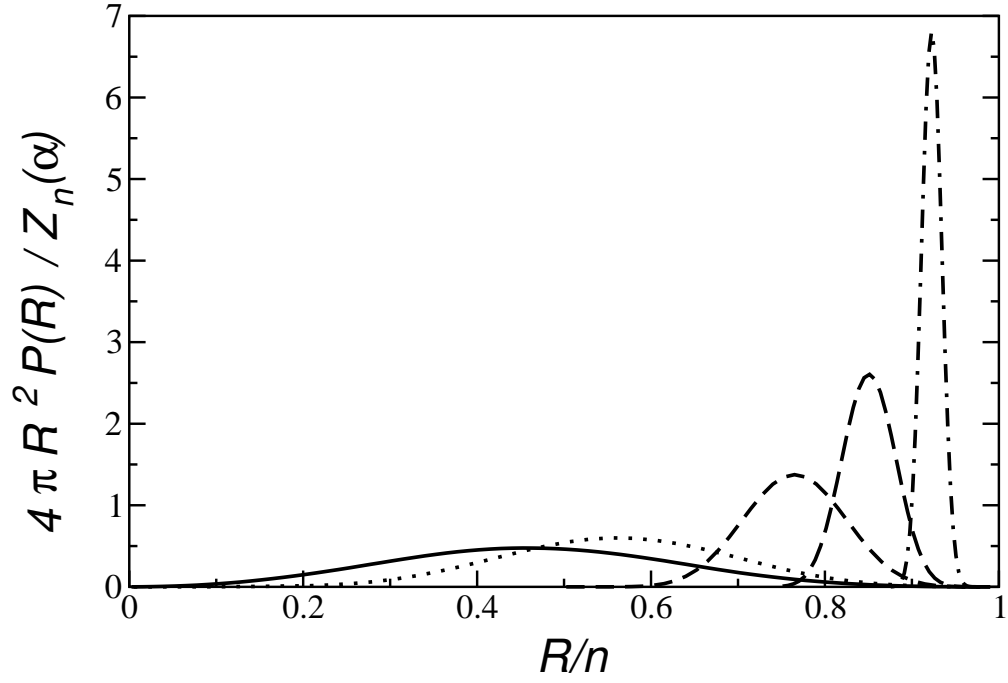


FIG. 1. Normalized polymer propagator $4\pi R^2 P(R)/Z_n(\alpha)$ versus R/n for $n = 5$. Continuous line ($\alpha = 0.33$), dotted line ($\alpha = 1.0$), dashed line ($\alpha = 3.0$), long dashed line ($\alpha = 5.0$) and dashed-dotted line ($\alpha = 10.0$).

Comment: Figure 1, First Author: Marcelo Marucho, Journal PRE

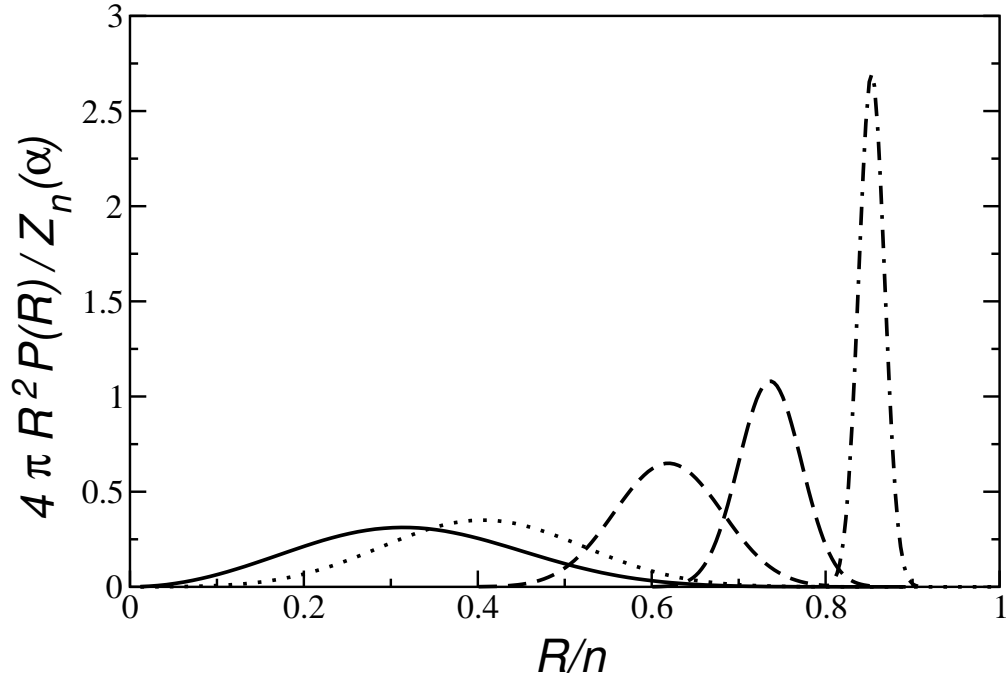


FIG. 2. Normalized polymer propagator $4\pi R^2 P(R)/Z_n(\alpha)$ versus R/n for $n = 10$. Continuous line ($\alpha = 0.33$), dotted line ($\alpha = 1.0$), dashed line ($\alpha = 3.0$), long dashed line ($\alpha = 5.0$) and dashed-dotted line ($\alpha = 10.0$).

Comment: Figure 2, First Author: Marcelo Marucho, Journal PRE

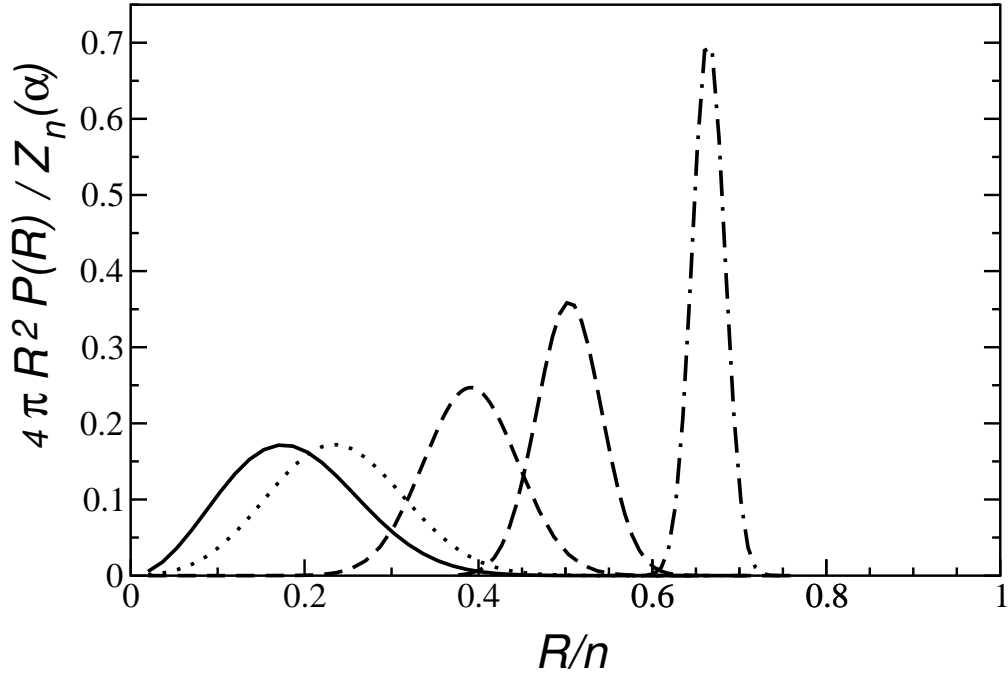


FIG. 3. Normalized polymer propagator $4\pi R^2 P(R)/Z_n(\alpha)$ versus R/n for $n = 30$. Continuous line ($\alpha = 0.33$), dotted line ($\alpha = 1.0$), dashed line ($\alpha = 3.0$), long dashed line ($\alpha = 5.0$) and dashed-dotted line ($\alpha = 10.0$).

Comment: Figure 3, First Author: Marcelo Marucho, Journal PRE

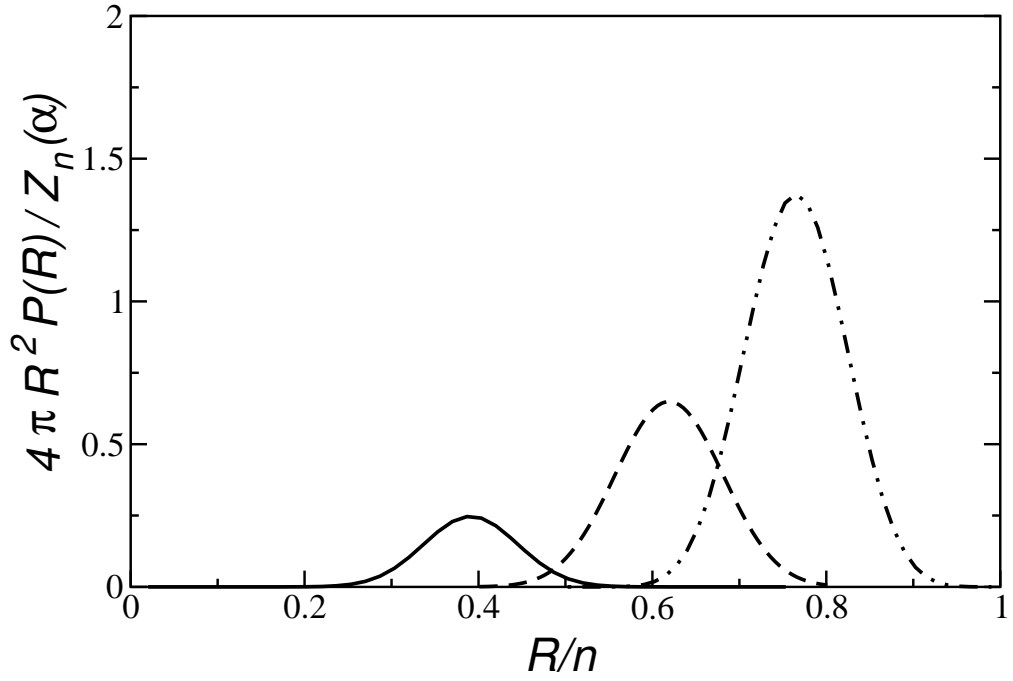


FIG. 4. Normalized polymer propagator $4\pi R^2 P(R)/Z_n(\alpha)$ versus R/n for $\alpha = 3.0$. Continuous line ($n = 30$), dashed line ($n = 10$) and dashed-dotted line ($n = 5$).

Comment: Figure 4, First Author: Marcelo Marucho, Journal PRE

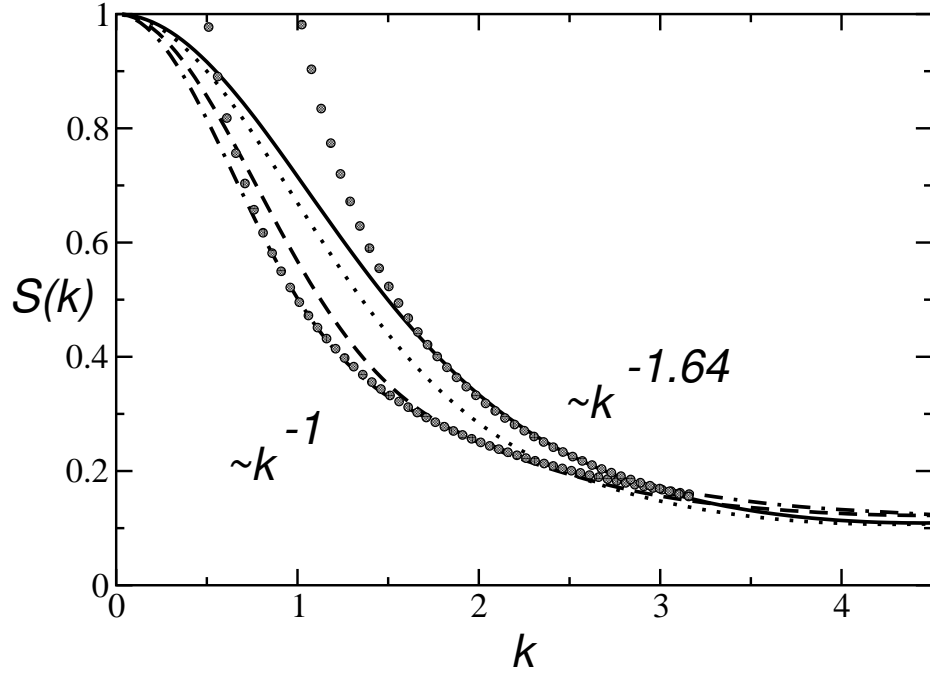


FIG. 5. Single chain structure factor $S(k; n; \alpha)$ versus wave vector k for $n = 5$. Continuous line ($\alpha = 0.33$), dotted line ($\alpha = 1.0$), dashed line ($\alpha = 3.0$), dashed-dotted line ($\alpha = 10.0$) and circles (best fits to the power law in the range $k \in [2, 3]$ for $\alpha = 0.33$ and $\alpha = 10.0$).

Comment: Figure 5, First Author: Marcelo Marucho, Journal PRE

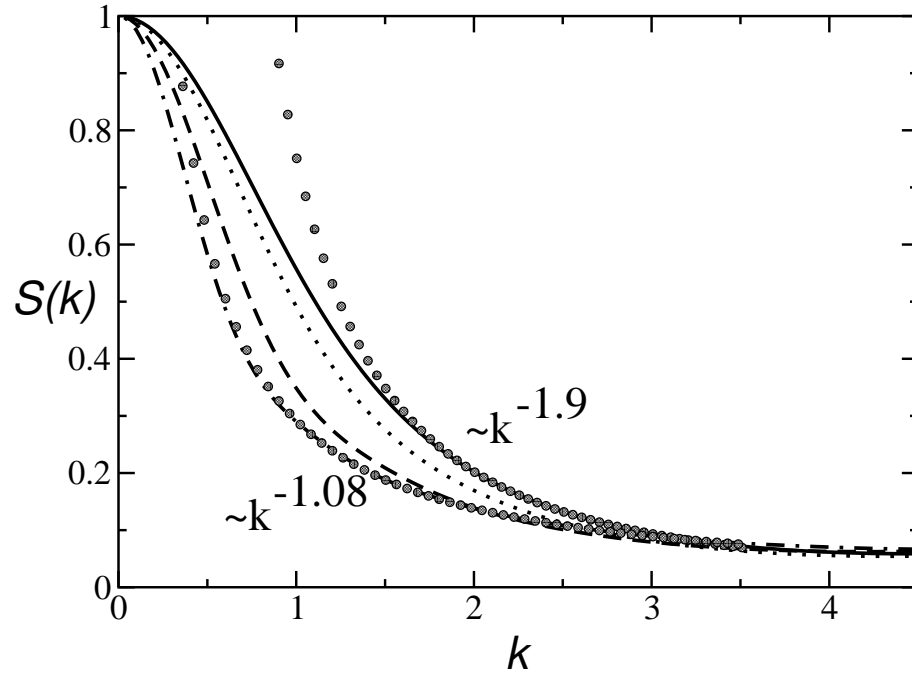


FIG. 6. Single chain structure factor $S(k; n; \alpha)$ versus wave vector k for $n = 10$. Continuous line ($\alpha = 0.33$), dotted line ($\alpha = 1.0$), dashed line ($\alpha = 3.0$), dashed-dotted line ($\alpha = 10.0$) and circles (best fits to the power law in the range $k \in [2, 3]$ for $\alpha = 0.33$ and $\alpha = 10.0$).

Comment: Figure 6, First Author: Marcelo Marucho, Journal PRE

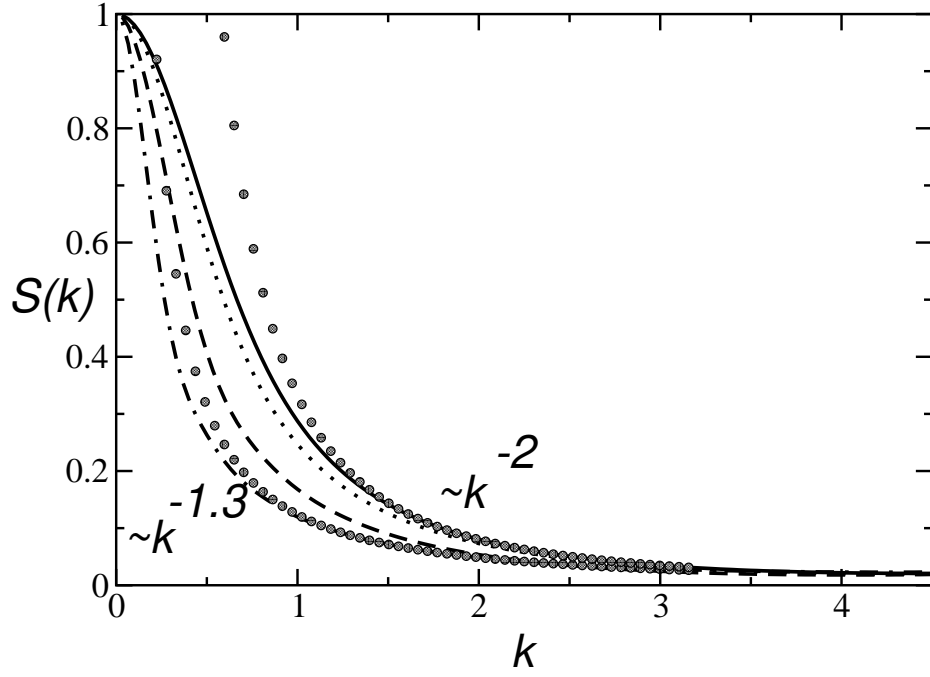


FIG. 7. Single chain structure factor $S(k; n; \alpha)$ versus wave vector k for $n = 30$. Continuous line ($\alpha = 0.33$), dotted line ($\alpha = 1.0$), dashed line ($\alpha = 3.0$), dashed-dotted line ($\alpha = 10.0$) and circles (best fits to the power law in the range $k \in [2, 3]$ for $\alpha = 0.33$ and $\alpha = 10.0$).

Comment: Figure 7, First Author: Marcelo Marucho, Journal PRE

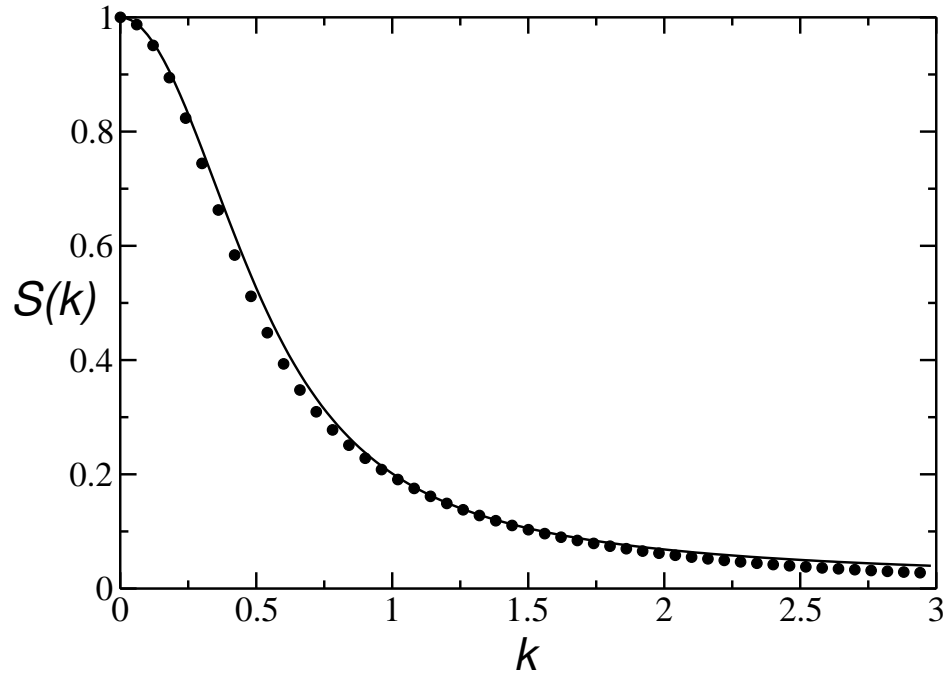


FIG. 8. Single chain structure factor $S(k; n; \alpha)$ versus wave vector k for $n = 30$. (Line) Kholodenko's model with $\alpha = 1$, (points) this work with $\alpha = 2$.

Comment: Figure 8, First Author: Marcelo Marucho, Journal PRE

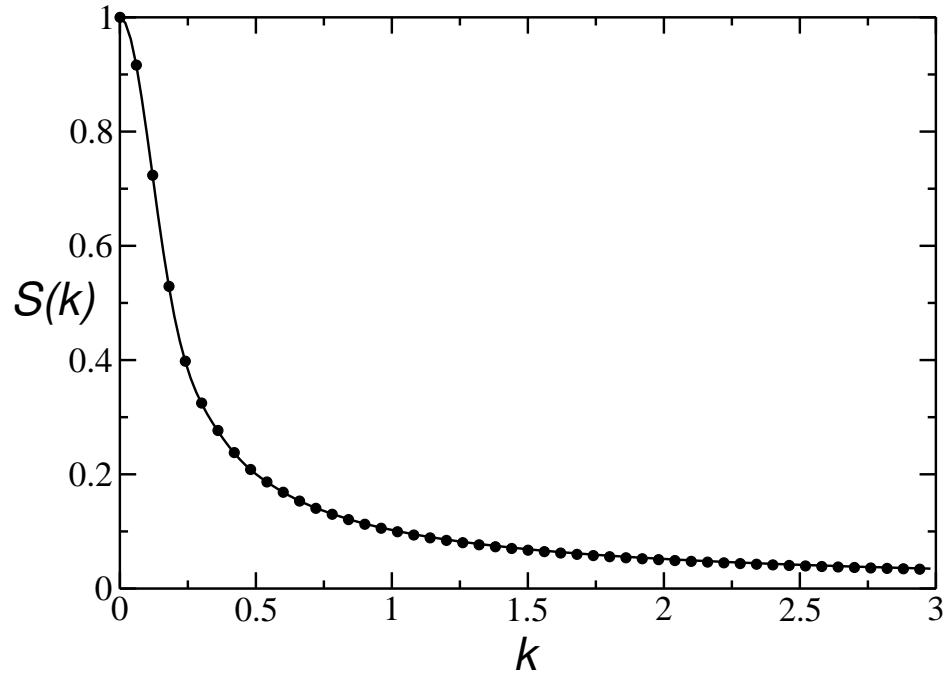


FIG. 9. Single chain structure factor $S(k; n;)$ versus wave vector k for $n = 30$. (Line) Kholodenko's model with $a = 50$, (points) this work with $n = 100$.

Comment: Figure 9, First Author: Marcelo Marucho, Journal PRE

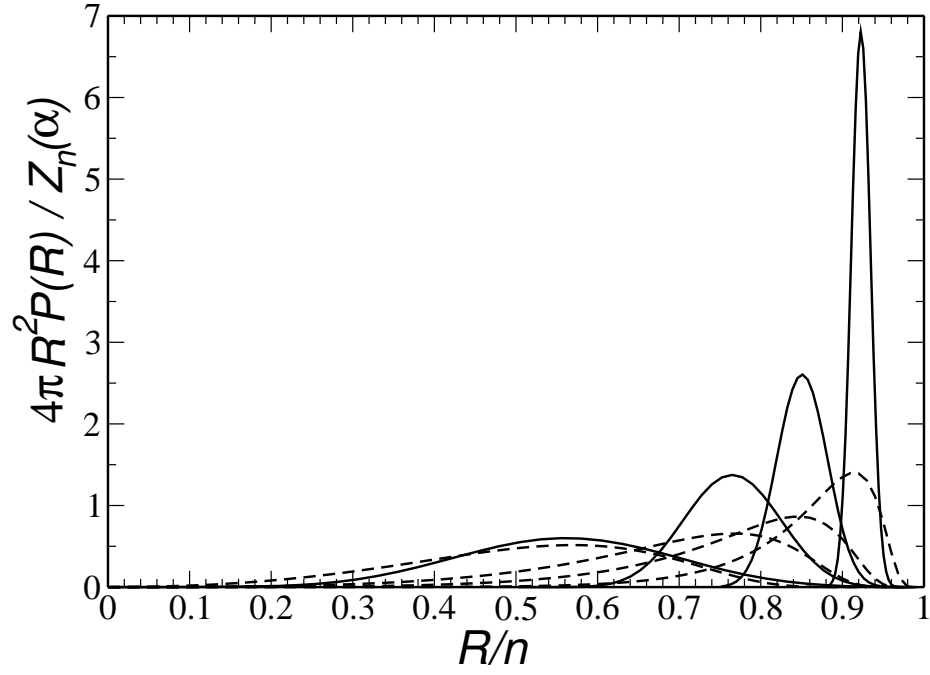


FIG. 10. Normalized polymer propagator $P(R; n; \alpha)$ versus end-to-end distance R in units of Kuhn length for $n = 5$. (Continuous lines) this work, (dashed lines) Wilhelm and Frey's results.

Comment: Figure 10, First Author: Marcelo Marucho, Journal PRE